

One-dimensional Onsager theory for carrier injection in metal-insulator systems

Daniel F. Blossey

Xerox Webster Research Center, Webster, New York 14580

(Received 16 November 1973)

A one-dimensional Onsager theory is developed to explain the field and temperature dependence of internal photoemission in metal-insulator systems.

Internal photoemission has been used largely for determination of barrier heights for carrier injection in metal-insulator systems.^{1,2} The technique is very similar to photoemission from metals into vacuum, except that the hot carriers (electrons *and* holes) are injected from the metal directly into the transport bands of the insulator. In the absence of Fermi-level stabilization at the surface,³ the photoemission threshold is a direct measure of the energy separation of the Fermi level in the metal and the bottom (top) of the conduction (valence) band. Since the main emphasis has been on the spectroscopic location of injection barriers, only a few investigators^{4,5} have studied the details of the field and temperature dependence of the injection currents. Since the hot carriers are injected into a solid, instead of vacuum, they can lose energy through scattering events.⁴⁻⁶ Through backscattering, diffusion, or the attractive force of the image potential, some of the injected carriers will be returned to metal and will not be collected.⁴ The collection efficiency will be field dependent⁵ and should saturate at a field determined by the microscopic mobility of the injected carrier in the solid.¹ Only at very high fields are barrier-lowering effects observed⁷ and can tunneling effects be important as is the case in field-emission spectroscopy.⁸ In this paper we propose to develop a theory that describes the field and temperature dependence of the collection efficiency for injected carriers in metal-insulator systems and to show that this theory is in good agreement with internal photoemission experiments. We will also discuss the implications of these results on barrier determinations.

The general features of the injection process are shown schematically in Fig. 1 for the case of electron injection. After the hot carrier is injected into the solid, it will give up energy to the lattice and become thermalized at some distance from the metal surface. The thermalized carrier can then drift under the influence of diffusion, its own image field, and the applied field with the ultimate fate of either returning to the metal or being collected. The problem thus divides naturally into (a) a description of the

thermalization process and (b) collection of the thermalized carriers. The thermalization of hot carriers will be described in a phenomenological fashion, incorporating the microscopic mobility, whereas the motion after thermalization will be treated exactly. We will see that the microscopic mobility determines the thermalization length in the solid and that the collection efficiency is related to the microscopic mobility through the thermalization length. The carrier motion after thermalization will be treated first.

When one wishes to describe thermal-carrier motion in a combined Coulombic-plus-electric-field potential, the description is generally formed in the context of a Poole-Frenkel-⁹ or Onsager¹⁰-type formalism. The description of quantum-mechanical particles is, of course, quite different.¹¹ In comparing the Poole-Frenkel and Onsager treatments, one must conclude that the Onsager treatment is the correct first-principles treatment of this problem, whereas the Poole-Frenkel is, at best, superficial. The Poole-Frenkel treatment has been popularized mainly because of the simplicity of the resulting expression. This conclusion is further supported by the recent successes of the Onsager theory in explaining the field dependence of carrier photo-generation in such diverse solids as anthracene,¹² polymeric poly-*N*-vinylcarbazole-trinitrofluorenone (PVK-TNF) 1:1 complex,¹³ crystalline As₂S₃,¹⁴ and amorphous Se.¹⁵ The description of the carrier injection process is simply a one-dimensional analog to the carrier generation process in the bulk in which the thermalized carrier pair starts with an initial separation (thermalization length) and has the ultimate fate of either recombination or dissociation.

To describe the motion of thermal carriers, we will start with the continuity equation which, for steady-state currents, is given by

$$G(x) + \frac{d}{dx}(nv) = 0, \quad (1)$$

where $G(x)$ defines the rate and position at which the hot injected carriers are thermalized and acts as a source term for the thermal carriers; n is the thermal-carrier density and v is their velocity.

The velocity of the thermal carriers is governed by diffusion, the image force, and the applied field and is given by

$$v = -\frac{D}{n} \frac{dn}{dx} - \mu \frac{d\phi}{dx}, \tag{2}$$

where $D = \mu kT/e$ is the diffusion coefficient, μ is the carrier mobility, and the potential $e\phi$ is given by

$$e\phi = -(e^2/4\epsilon x) - e\mathcal{E}x, \tag{3}$$

the first term being the image-force potential and the second the applied-field potential. Combining (1) and (2) we have that

$$\frac{e}{\mu kT} G(x) = \frac{d}{dx} \left\{ \exp\left(-\frac{e\phi}{kT}\right) \frac{d}{dx} \left[n \exp\left(\frac{e\phi}{kT}\right) \right] \right\}. \tag{4}$$

If there are sinks at both the origin (emitter) and infinity (collector) and if the potential $e\phi$ becomes large negative at these points, the collected current will have the form

$$J = \int_0^\infty dx eG(x)P(x), \tag{5}$$

where Eq. (5) was obtained by integrating (4) twice, changing variables, and calculating the current $J = nev$ at infinity.¹⁶ The function $P(x)$ is simply

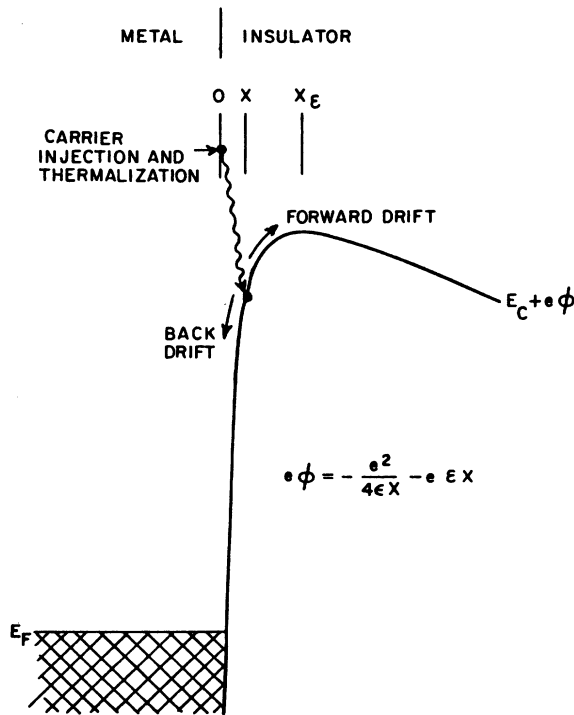


FIG. 1. Schematic of collection process for injected hot electrons in metal-insulator system.

the escape probability for a thermal carrier with initial position x and is given by

$$P(x) = \frac{\int_0^x dx \exp(e\phi/kT)}{\int_0^\infty dx \exp(e\phi/kT)}. \tag{6}$$

The function $P(x)$ has the correct limiting values of $P = 1$ for an initial position of infinity and $P = 0$ for an initial position at $x = 0$. For the potential given in (3) the definite integral can be evaluated as¹⁷

$$\int_0^\infty dx \exp\left(\frac{-e^2}{4\epsilon x kT} - \frac{e\mathcal{E}x}{kT}\right) = 2x_\delta k_1(\xi), \tag{7}$$

where $x_\delta = \frac{1}{2}(e/\epsilon\mathcal{E})^{1/2}$ is the position of the maximum in $e\phi$, k_1 is a first-order modified Bessel function, and $\xi = (e^3\mathcal{E}/\epsilon k^2 T^2)^{1/2}$. The escape probability P is shown as a function of dimensionless field at constant temperature in Fig. 2 for a series of initial dimensionless starting positions. A typical value of \mathcal{E}_T at room temperature would be

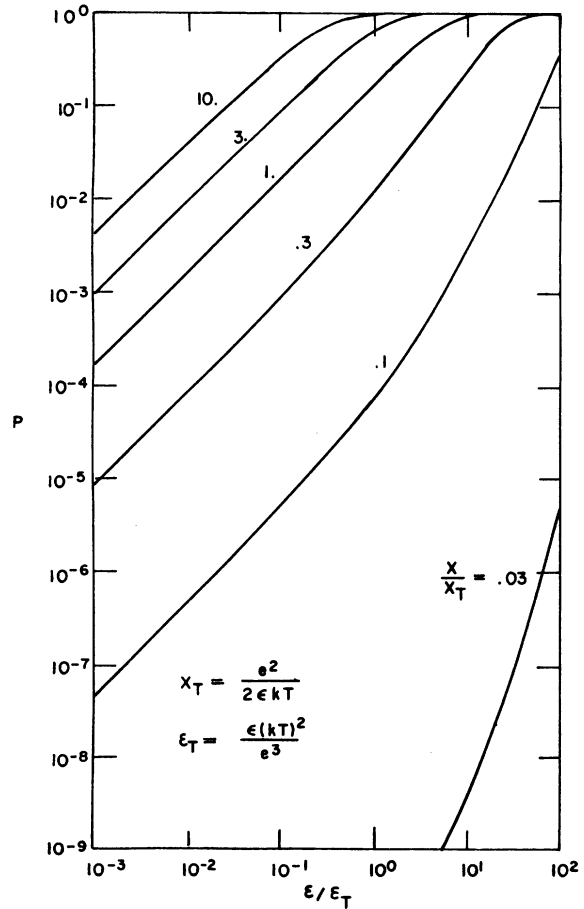


FIG. 2. Constant-temperature escape probabilities of thermal carriers from their own image potential as a function of dimensionless electric field for a series of initial positions.

10^4-10^5 V/cm for most solids, a typical value for x_T would be 10-100 Å. The fact that P goes linearly to zero with field is strictly a result of the dimensionality of the potential. For a three-dimensional potential, P approaches a nonzero value at zero field, a result which has been substantiated experimentally.¹⁸ Mathematically, it is significant that the three-dimensional potential is divergence free, whereas the one-dimensional potential is

$$2x_\delta k_1(\xi) \sim kT/e\mathcal{E}, \text{ small } \mathcal{E}, \text{ large } T, \\ \sim \left(\frac{\pi^2 k^2 T^2}{4\epsilon e \mathcal{E}^3}\right)^{1/4} \exp\left(\frac{-(e^3 \mathcal{E}/\epsilon)^{1/2}}{kT}\right), \text{ large } \mathcal{E}, \text{ small } T.$$

It is important to point out that the saturation field (the field at which $P \rightarrow 1$) is not a direct function of the mobility but instead depends on the thermalization length which, in turn, is dependent on the microscopic mobility. The temperature dependence of P is shown on Fig. 3 at constant field. For small thermalization lengths, $x < x_\delta$, P is thermally activated. At very high temperatures, rapid back diffusion causes P to decrease, which is observed experimentally.⁶

To calculate thermalization lengths let us start with the equation of motion for an injected hot carrier,

$$m \frac{dv}{dt} = m v \frac{dv}{dx} = -\frac{ev}{\mu} - e \frac{d\phi}{dx}, \quad (8)$$

where we take the velocity of the particle to be an explicit function of x and the energy-loss scattering process is included phenomenologically as a mobility-dependent drag term.¹⁹ Upon thermalization the acceleration term is negligible and (8) reduces to (2) without the diffusion term. We have assumed in (8) that the main forces in the deceleration of the hot carriers are the potential and drag terms and have neglected diffusion. The condition for thermalization is taken to be when the carrier's kinetic energy, $\frac{1}{2}mv^2$, equals $\frac{1}{2}kT$ (one degree of freedom). The above equation is nonlinear and has to be solved numerically. For very hot carriers ($E_n \gg E_0 + E_f$), the thermalization length x is given by

$$x \approx \mu(m/e)v_0.$$

The kinetic energy $\frac{1}{2}mv_0^2$ is measured from the bottom of the conduction band where v_0 is the initial velocity of the injected carrier. Thus, the higher the microscopic mobility, the farther the carriers travel before thermalization. For small to medium fields and large x ,

$$P(x) \approx 1 - \exp(-e\mathcal{E}x/kT),$$

which means that the saturation field in this approx-

imation is not. A divergence-free potential allows $n = (\text{const})$ to be a solution of (4) everywhere. This is a field-independent solution, whereas for the potential given in (3) there are no field-independent solutions. The superlinear field behavior of P at high fields and short thermalization lengths is due to barrier lowering. The linear-field term and barrier lowering both come from different asymptotic forms of (7),

imation is

$$\mathcal{E}_{\text{sat}} \approx \frac{kT}{\mu m v_0}.$$

This expression has meaning only for high-mobility materials ($\mu > 100$ cm²/V sec) and is different from the standard expression for the saturation field.¹ The temperature dependence and the field magnitude are both in agreement with observation.⁵

To calculate the injection current J we must map the energy distribution of injected hot carriers

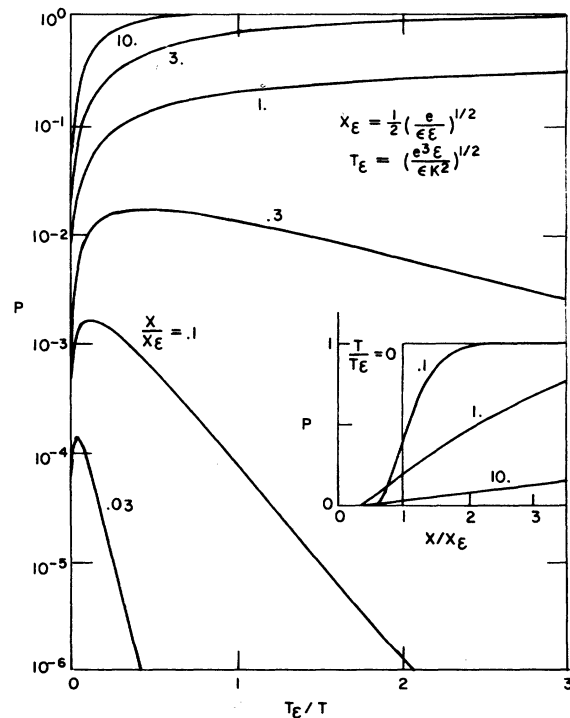


FIG. 3. Constant-electric-field escape probabilities of thermal carriers from their own image potential as a function of dimensionless inverse temperature for a series of initial positions. x_δ is the position of the potential maximum.

into the source term $G(x)$ in (5) by using (8). But first we must calculate the kinetic-energy distribution for the kinetic energy of hot carriers normal to the interface, E_n . For internal photoemission, the primary step is the creation of hot carriers in the metal. These hot carriers will have an equal probability of traveling in all directions, whereby only a certain fraction of the carriers will have enough kinetic energy normal to the surface to get in. The standard assumption for internal-photoemission calculations is that the transition matrix element in the metal does not change rapidly with photon energy over the region of interest.¹ This means that excitations between 0 and $h\nu$ above the Fermi level are equally probable. If this approximation is valid, it is easy to show that the differential yield [(carriers injected per photon) per normal kinetic energy] is given by

$$\frac{dY}{dE_n} = \frac{1}{2h\nu} \left[\left(\frac{h\nu + E_F}{E_n} \right)^{1/2} - 1 \right], \quad E_F < E_n < h\nu + E_F. \quad (9)$$

If the injection barrier (relative to E_F) is E_0 and scattering is neglected, integration of (9) between $E_F + E_0$ and $E_F + h\nu$ gives the standard field-independent result for the photoemission yield,

$$Y = 1 - \frac{1}{2} \left(\frac{h\nu - E_0}{h\nu + E_F} \right) - \left[1 - \left(\frac{h\nu - E_0}{h\nu + E_F} \right) \right]^{1/2} \\ \simeq \frac{1}{8} \left(\frac{h\nu - E_0}{h\nu + E_F} \right)^2. \quad (10)$$

Equation (10) has been used as the basis for barrier determination in that, by plotting the square root of the photoemission current vs photon energy near threshold; the threshold is determined by linear extrapolation of the curve to zero. To calculate the yield with scattering we combine (9), (8), and (5). Through (8) we calculate the thermalization length $x = x(E_n)$ as a function of the normal kinetic energy E_n . The yield $Y = J/eF$, where F is the photon flux, is defined as

$$Y = \int_{E_F}^{h\nu + E_F} dE_n \frac{dY}{dE_n} P[x(E_n)], \quad (11)$$

where we have described the source term as $G(x) = (dY/dE_n)(dE_n/dx)$ and inserted this into (5).

This equation must be solved numerically. Comparison between theory and experiment⁵ is shown for electron injection in Cu:CdS system in Fig. 4a and for hole injection in Au:Se system in Fig. 4b. The microscopic mobilities of 300 cm²/V sec for CdS and 20 cm²/V sec were chosen for best fits and agree quite well with crystalline values for both CdS²⁰ and Se.²¹ The collected charge was

in arbitrary units. The above theory allows for a much higher microscopic mobility for Se than is required in simpler theories.⁵ For low-mobility solids ($\mu \ll 100$ cm²/V sec) saturation will occur above 10⁶ V/cm,²² a field region where barrier-lowering effects are also important.⁷ The field dependencies shown in Fig. 4 are largely determined by which curve in Fig. 2 the hottest carriers fall onto.

For high-mobility materials at low fields, we can approximate

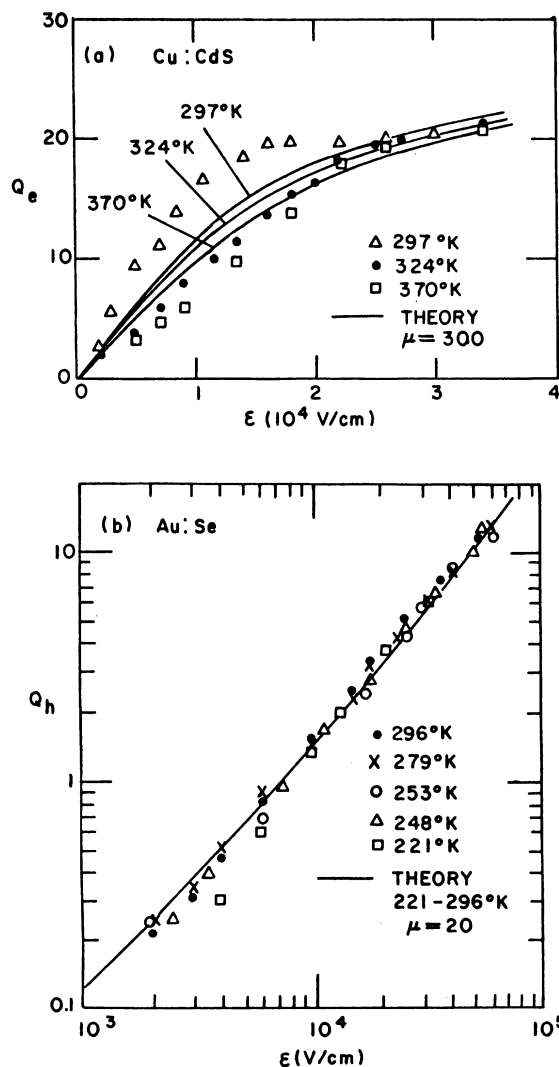


FIG. 4. Comparison of theory and experiment (after Mort, Schmidlin, Lakatos, Ref. 5) for (a) electron injection in Cu:CdS system and (b) hole injection in Au:Se system. The collected charge, Q_e and Q_h , are in arbitrary units and the microscopic mobilities, 300 cm²/V sec for CdS and 20 cm²/V sec for amorphous Se, are chosen to fit the data.

$$P[x(E_n)] \simeq 0, E_n < E_0 + E_F$$

$$\simeq (\mu \mathcal{E} / kT) [2m(E_n - E_0 - E_F)]^{1/2},$$

$$E_n > E_0 + E_F,$$

whereby the yield may be calculated to be

$$Y \simeq \frac{\mu \mathcal{E}}{kT} \frac{(2m)^{1/2}}{15} \frac{(E_0 + E_F)^{3/2}}{h\nu} \left(\frac{h\nu - E_0}{h\nu + E_F} \right)^{5/2},$$

$$\mathcal{E} < \mathcal{E}_{\text{sat}}. \quad (12)$$

For $\mathcal{E} > \mathcal{E}_{\text{sat}}$, the photoemission yield is given by (10). Equation (12), even though it is limited to high-mobility solids ($\mu > 100 \text{ cm}^2/\text{V sec}$), demonstrates that bulk scattering can cause a change in the threshold power law ($2 - \frac{5}{2}$). In the absence of

a known power law, it is suggested that peaks in the wavelength-modulation spectrum, plotting $(1/J)[dJ/d(h\nu)]$, should give the most precise measure of barrier heights.

In summary, we have shown how field and temperature dependencies can arise in internal photoemission and have obtained quantitative agreement with experiment. We evaluate explicitly the escape probability of a thermal carrier from its image potential and show how the microscopic mobility can be incorporated into the theory. We argue that scattering causes changes in the threshold power law and suggest wavelength-modulation spectroscopy as the recommended method for precise barrier determination.

- ¹For a review of the field up to 1968, see R. Williams, in *Semiconductors and Semimetals*, edited by R. K. Williams and A. C. Beer (Academic, New York, 1970), Vol. 8.
- ²C. A. Mead, *Solid-State Electron.* **9**, 1023 (1966).
- ³S. Kurtin, T. C. McGill, and C. A. Mead, *Phys. Rev. Lett.* **22**, 1433 (1969).
- ⁴C. R. Crowell and S. M. Sze, *Solid-State Electron.* **9**, 1035 (1966).
- ⁵J. Mort, F. W. Schmidlin, and A. I. Lakatos, *J. Appl. Phys.* **42**, 5761 (1971).
- ⁶E. M. Conwell, *Solid State Physics*, Suppl. 9 (Academic, New York, 1967).
- ⁷S. M. Sze, C. R. Crowell, and D. Kahng, *J. Appl. Phys.* **35**, 2534 (1964).
- ⁸J. W. Gadzuk and E. W. Plummer, *Rev. Mod. Phys.* **45**, 487 (1973).
- ⁹J. Frenkel, *Phys. Rev.* **54**, 657 (1938).
- ¹⁰L. Onsager, *Phys. Rev.* **54**, 554 (1938); *J. Chem. Phys.* **2**, 599 (1934).
- ¹¹D. F. Blossey, *Phys. Rev. B* **2**, 3976 (1970); *Phys. Rev. B* **3**, 1382 (1971).
- ¹²R. H. Batt, C. L. Braun, and J. F. Hornig, *J. Chem. Phys.* **49**, 1967 (1968); *Appl. Opt. Suppl.* **3**, 20 (1969).
- ¹³P. J. Melz, *J. Chem. Phys.* **51**, 1694 (1972).
- ¹⁴D. F. Blossey and R. Zallen, *Phys. Rev. B* **9**, 4306 (1974).
- ¹⁵D. M. Pai and R. C. Enck (unpublished).
- ¹⁶The major differences between this theory and that given in Ref. 5 are the same as the differences between Poole-Frenkel and Onsager theories for carrier photo-generation. In Poole-Frenkel theory, one must insert

- a loss (recombination) rate to compete with the emission rate, so that the resulting expression will not exceed unit quantum efficiency at high fields (above the saturation field). In Onsager theory, the recombination process is included naturally by placing a sink at the origin and allowing carriers to drift toward it in accordance with the continuity equation (Langevin recombination).
- ¹⁷*Handbook of Mathematical Functions*, edited by M. Abramowitz and I. A. Stegun (Dover, New York, 1965), p. 1028.
- ¹⁸R. C. Enck, *Phys. Rev. Lett.* **31**, 220 (1973).
- ¹⁹The treatment of the scattering of hot carriers is a very difficult problem (see Ref. 6). Rather than writing expressions in terms of electron-phonon coupling constants, final density of states, etc., we have chosen to parametrize the energy-loss process as a mobility-dependent drag term, this mobility being a parameter which is representative of the scattering processes in the band. Equation (8) should be valid if the carrier mean free path is small compared to the extent of the potential x_g . Since it is only at small fields (large x_g) that field dependencies are important, we argue that the region of validity for (8) is self-defining in that it is valid for $\mathcal{E} < \mathcal{E}_{\text{sat}}$ and it does not enter into the problem for $\mathcal{E} > \mathcal{E}_{\text{sat}}$.
- ²⁰W. E. Spear and J. Mort, *Proc. Phys. Soc. Lond.* **81**, 123 (1963).
- ²¹J. Mort, *J. Appl. Phys.* **39**, 3543 (1968); *Phys. Rev. Lett.* **18**, 540 (1967).
- ²²A. M. Goodman, *Phys. Rev.* **144**, 588 (1966).